RSC Advances

ROYAL SOCIETY OF CHEMISTRY

www.rsc.org/advances

Journal Name

RSCPublishing

ARTICLE

Exploiting oriented attachment in stabilizing La^{3+}-doped gallium oxide nano-spindles

Cite this: DOI: 10.1039/xoxxoooooox

M. Ibrahim Dar,[a,b] S. Sampath,[c] and S. A. Shivashankar*[a,b]

Received ooth January 2012,
Accepted ooth January 2012

DOI: 10.1039/xoxxoooooox

www.rsc.org/

Retaining the morphology of gallium oxide nanostructures during structural transformations or after doping with lanthanide ions is not facile. Here we report on the sonochemical synthesis of nearly monodisperse ~550 nm-long nano-spindles of undoped and La-doped α-GaOOH. The transformation of as-prepared undoped and La-doped α-GaOOH powders into corresponding undoped and La-doped Ga_2O_3 phases (α and β) was achieved by carrying out controlled annealing at elevated temperatures under optimized conditions. The formation of gallium oxide nano-spindles is explained by invoking the phenomenon of oriented attachment, as amply supported by electron microscopy. Interestingly, the morphology of the gallium oxide nano-spindles remained conserved even after doping them with more than 1.4 at.% of La^{3+} ions. Such robust structural stability could be attributed to oriented attachment-type of growth observed in the nano-spindles. The as-prepared samples and the corresponding annealed ones were thoroughly characterized by powder X-ray diffraction (PXRD), electron microscopy (SEM, TEM, and STEM-EDS) and X-ray photoelectron spectroscopy (XPS). Finally, photoluminescence from the single-crystalline undoped and La-doped β-Ga_2O_3 was explored.

Introduction

Gallium oxides have prompted much research interest, especially in the field of gas sensing, catalytic, and optoelectronic devices.[1,2,3] Ga_2O_3 exists in five different polymorphs, *viz.*,α, β, γ, δ, and ε.[4] Among these polymorphs, β-Ga_2O_3 is thermodynamically the most stable polymorph and crystallizes in a monoclinic structure. All other polymorphs are metastable, and on annealing at elevated temperatures, transform into β-Ga_2O_3.

For the synthesis of Ga_2O_3 nanostructures various methods have been adopted, most of which employ α-GaOOH nanostructures as precursor.[5] Laubengayer *et al.* were the first to report an experimental study on the transformation of gallium oxide polymorphs and hydroxides over the temperature range of 110°C to 1000°C.[6] With a wide band gap of 5.3 eV at room temperature, α-GaOOH exists in an orthorhombic structure and for its synthesis, hydrolysis,[7] sol–gel,[8] hydrothermal,[9] and sonochemical[10] methods have been employed. Additionally, a low temperature process has also been developed for the synthesis of α-GaOOH using the protein filament as a template and a catalyst.[11] Although the sonochemical method has emerged over the years as a versatile alternative to other solution-based methods for the synthesis of nanomaterials;[12] it has been scarcely used for the synthesis of gallium oxide nanostructures. Gedanken *et al.* documented the formation of cylindrical structures of GaOOH containing a gallium metallic core by sonicating an aqueous solution of $GaCl_3$ for 6 h.[10] In sonochemical synthesis, molecules undergo a chemical reaction due to the application of powerful ultrasound radiation in the frequency range of ~20 kHz – 10 MHz. Different theories have been put forth to explain how sonochemical reactions occur and all of them conclude that the formation, growth, and implosive collapse of bubbles in a liquid irradiated with ultrasound generate high local temperatures and pressures.[13]

Furthermore, α-GaOOH nanostructures with a variety of morphologies, including rod-like and scroll-like cylindrical structures, have also been fabricated.[10,14] Retaining such morphology during structural transformations or after doping with lanthanide ions has been a challenge. Occasionally, the effect of heat treatment on the shapes has been marginal and the original morphology could be conserved while transforming GaOOH nanostructures into Ga_2O_3 nanostructures.[7] The effect of lanthanide doping on the structural and morphological stability of gallium oxide nanostructures is intriguing. Although much has been reported in the literature regarding lanthanide-doped gallium oxide nanostructures, most reports have focused on the luminescence properties of resulting nanomaterials.[15] However, achieving robust structural stability for lanthanide-doped gallium oxide nanostructures has been difficult. This is primarily due to the considerable difference in the ionic radii of

Ga^{3+} (0.62 Å) and Ln^{3+} (0.91 Å). Naidu *et al.* studied the effect of Ln^{3+} (Eu^{3+}, Tb^{3+}, and Dy^{3+}) on the structural stability of layered GaOOH and concluded on the basis of structural and vibrational studies that the layered structure collapses when >1 at.% of Ln^{3+} is added to the reaction mixture.[16] Another problem associated with lanthanide-doped gallium oxide is the formation of a secondary phase after annealing at elevated temperatures. For example, Li *et al.* observed the formation of the garnet phase, $Dy_3Ga_5O_{12}$, along with Ga_2O_3:Dy, upon decomposition of GaOOH:Dy^{3+} (3%) under heat treatment.[17]

To gain fundamental understanding of properties of nanostructures, such as luminescence, they should be synthesized without employing any templates or growth-directing agents, especially by adopting simple and scalable routes. We report here on a facile sonochemical route for the synthesis of undoped and La-doped α-GaOOH single crystalline nano-spindles that is scalable and employs no growth-controlling or -directing agent. The transformation of as-prepared α-GaOOH single crystalline nanostructures into Ga_2O_3 phases (α and β) was achieved by carrying out controlled annealing at elevated temperatures, under optimized conditions. Remarkably, morphology of the gallium oxide nano-spindles remained conserved even after doping them with La^{3+} ions (>1.4 at.%) and during structural transformations. The as-prepared samples and the corresponding annealed ones were thoroughly characterized by powder X-ray diffraction (PXRD), electron microscopy (SEM, TEM, and STEM-EDS) and X-ray photoelectron spectroscopy (XPS). Furthermore, room temperature photoluminescence spectra (colloid) of single crystalline, undoped and La-doped β-Ga_2O_3 nano-spindles have also been studied.

Results and discussion

Single-crystalline undoped and La-doped *α*-GaOOH nano-spindles were synthesized using the growth directing or controlling agent free ultrasonic-assisted, bottom-up approach.

Structural characterization of La-doped and undoped Ga-oxides nanostructures

All observed peaks in the powder XRD patterns obtained from as-prepared La-doped (**Fig. 1a**) and undoped (**ESI)** gallium oxide samples can be indexed to the orthorhombic structure of *α*-GaOOH (JCPDS number # 06-0180). Dehydrating La-doped and undoped *α*-GaOOH nanostructures at 500 °C under ambient conditions transformed them, respectively, into nano-spindles of La-doped and undoped *α*-Ga_2O_3, as shown clearly by XRD (**Fig. 1b & ESI**). All observed peaks in the powder XRD patterns can be indexed to the rhombohedral structure of *α*-Ga_2O_3 (JCPDS number # 43-1013).The *α*-Ga_2O_3 obtained above was employed as the precursor for the synthesis of the *β*-Ga_2O_3 phase, as documented in the literature (equation 1).[18]

$$GaOOH \xrightarrow[>500\ ^{\circ}C]{} \alpha - Ga_2O_3 \xrightarrow[>750\ ^{\circ}C]{} \beta - Ga_2O_3 \quad equation\ 1$$

These transformations are irreversible under ambient conditions and have been well studied. The first transformation, i.e., from *α*-GaOOH to *α*-Ga_2O_3, can be achieved at a moderate temperature of ~ 500 °C, presumably due to the involvement of the dehydration process. However, the phase transformation from hexagonal α-Ga_2O_3 to monoclinic β-Ga_2O_3 requires a more elevated temperature of ~ 800 °C, as the two crystal structures are completely different. The formation of β-Ga_2O_3 was confirmed by powder XRD, as all observed peaks in the respective powder XRD patterns (**Fig. 1c & ESI**) can be indexed to the monoclinic structure of β-Ga_2O_3 (JCPDS number # 41-1103). It is to be noted that all the phases obtained are pure to within the detection limit of XRD, as no peak corresponding to any other impurity phase was observed in either the sample of pure or La-doped gallium oxide nano-spindles. Furthermore comparative analysis of XRD patterns (**ESI**) of pure and La-doped β-Ga_2O_3 samples reveals a shift in the peak positions which could be attributed to the presence of La^{3+} in the lattice.

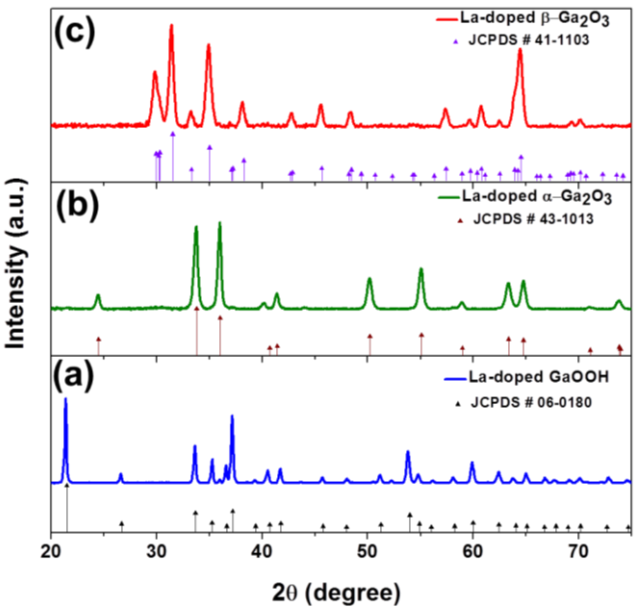

Fig. 1 Powder X-ray diffraction patterns of La-doped gallium oxides nano-spindles

Morphological characterization: Electron microscopy

To analyze the morphology, undoped *α*-GaOOH and La-doped *α*-GaOOH samples were examined by field emission scanning electron microscopy (FESEM). Low-magnification imaging (**Fig. 2a, b**) shows the presence of nearly monodisperse *α*-GaOOH nano-spindles with an extension of ~550 nm along the longer dimension. The high-magnification FESEM images (**Fig. 2a, b, inset**) reveal that both undoped *α*-GaOOH and La-doped *α*-GaOOH are ostensibly composed of fine nanoparticles. The nano-spindles seem to be composed of considerably small nanoparticles is in apparent discord with the sharp peaks observed in the powder X-ray diffraction (XRD) patterns. Therefore, to unravel the details, we examined the nano-spindles by transmission electron microscopy (TEM).

TEM was employed to study the crystallinity, morphology, size, and size dispersion of the synthesized undoped *α*-GaOOH, La-doped *α*-GaOOH, and their corresponding annealed nanostructures. The bright-field TEM images (BF-TEM) of both undoped *α*-GaOOH (**Fig. 3a**) and La-doped *α*-GaOOH (**Fig. 4a**) display the presence of individual nano-spindles with an average length of 550 nm and diameter 260 nm. High-resolution TEM image (**Fig. 3b & 4b**) reveals crystal lattice fringes with *d* spacing of 2.4 Å and 2.6 Å, corresponding, respectively, to the (111) and (130) planes of orthorhombic *α*-

GaOOH. The selected-area electron diffraction (SAED) patterns obtained for both undoped α-GaOOH **(Fig. 3c)** and La-doped α-GaOOH **(Fig. 4c)** show bright spots which correspond perfectly to the orthorhombic structure of α-GaOOH, thus bring out the single crystalline nature of nano-spindles. From comparative TEM analysis of undoped and doped α-GaOOH, we conclude that there is no effect of La^{3+} insertion on the morphology of α-GaOOH and the single crystalline nature remained conserved remarkably well.

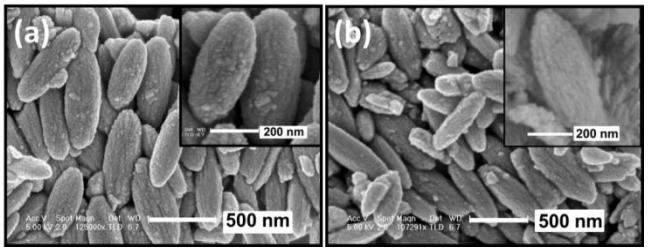

Fig. 2 FESEM micrographs of (a) undoped α-GaOOH and (b) La-doped α-GaOOH nano-spindles

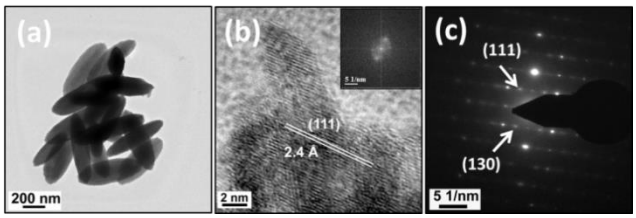

Fig. 3 Undoped α-GaOOH nano-spindles: (a) Bright-field TEM image; (b) HRTEM (inset: FFT pattern) and (c) SAED pattern

Similarly, annealed samples were examined by TEM. The bright-field TEM images (BF-TEM) of undoped β-Ga_2O_3 and La-doped β-Ga_2O_3 **(see ESI)** display the presence of individual nano-spindles with an average length and diameter of 550 nm and 250 nm, respectively. The SAED patterns obtained for undoped β-Ga_2O_3 and La-doped β-Ga_2O_3 **(see ESI)** show bright spot patterns that correspond perfectly to monoclinic β-Ga_2O_3, thus corroborating the XRD data.

In summary, TEM analysis brings out that harsh heat treatment does not affect the morphologies of undoped β-Ga_2O_3, and La-doped β-Ga_2O_3, as their nano-spindle type morphology remains intact during structural transformations.

It is well known that the distribution of constituent elements strongly influences the properties of the doped nanostructures. Therefore, detailed compositional and atomic distribution analysis of La-doped α-GaOOH nanostructures becomes imperative and was carried out by performing EDS mapping under the STEM mode. Line scans of La-doped α-GaOOH nano-spindles reveal the homogeneous distribution of the constituent atoms, i.e., La, Ga, and O, across the dimensions of the nano-spindles (**Fig. 4d**). Similarly, area-mapping reveals the uniform distribution of the constituent atoms, i.e., La, Ga, and O, throughout the dimensions of the nanostructures (**Fig. 4e-g**). We envisage that the formation of homogeneous La-doped α-GaOOH nano-spindles was facilitated by the uniform presence of the sonic field throughout the volume of the reaction mixture.

EDX and XPS analysis

For determining La^{3+} quantitatively, the La-doped GaOOH sample was examined by energy-dispersive X-ray spectroscopy under the STEM mode (STEM-EDS) (**Fig. 5**). Quantification of point-EDS spectrum (**Fig. 5**) obtained from an individual La-doped α-GaOOH nano-spindle showed the proportion of La ions to be ~1.45 at.%. It is noteworthy that morphology of these La-doped α-GaOOH nano-spindles containing ~1.45 at.% of La was found to be stable. This renders our present approach for the synthesis of La-doped α-GaOOH nano-spindles distinctive.

Furthermore, X-ray photoelectron spectroscopy (XPS) was used for the chemical analysis of La-doped α-GaOOH nano-spindles. Fig. 6a, b shows the core shell XPS spectra of Ga-2p and La-3d levels recorded from La-doped α-GaOOH nano-spindles. The two strong peaks (**Fig. 6a**) observed at 1120.1 eV and 1147.1 eV are in agreement with the binding energies of Ga $2p_{3/2}$ and Ga $2p_{1/2}$, respectively.[19] The core shell La-3d spectrum (**Fig. 6b**) shows sub-splitting of La-$3d_{3/2}$ and La-$3d_{5/2}$ peaks around (857.91 eV, 854.50 eV) and (840.70 eV, 837.53 eV), respectively.[20]

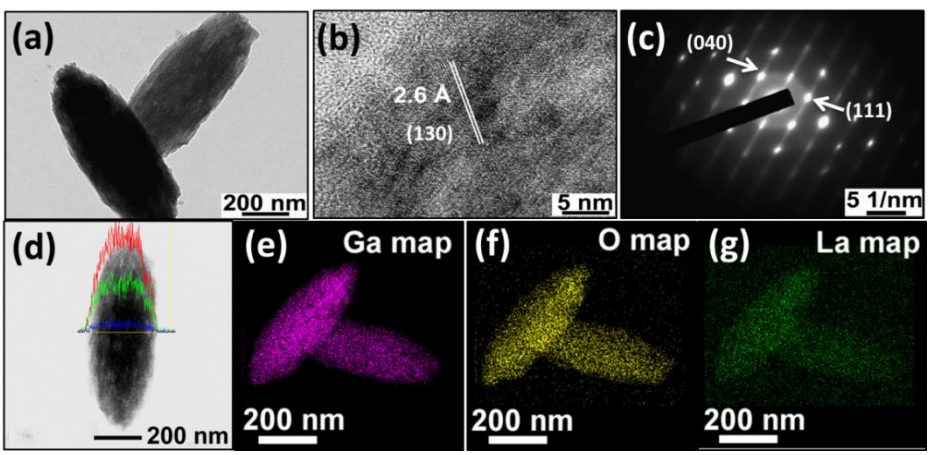

Figure 4: La-doped α-GaOOH nano-spindles: (a) Bright-field TEM image; (b) HRTEM (c) SAED pattern. (d) STEM bright-field image with EDS line spectra (e) Area-mapping for Ga, (f) Area-mapping for O and (g) Area-mapping for La.

Journal Name RSCPublishing

ARTICLE

These observations, i.e., binding energy values for Ga-2p and La-3d, are in agreement with the literature and indicate the presence of trivalent states of both gallium and lanthanum in La-doped α-GaOOH. XPS data thus provide further evidence for the presence of La^{3+} in the La-doped α-GaOOH nano-spindles.

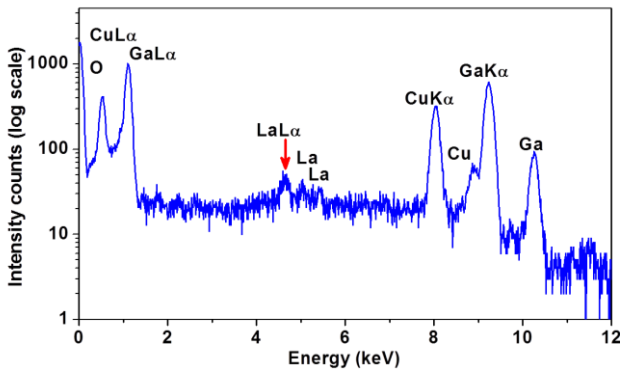

Fig. 5 Point EDS spectrum obtained from single La-doped α-GaOOH nano-spindle.

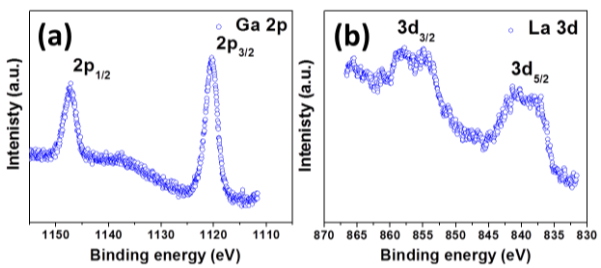

Fig. 6 X-ray photoelectron spectra of (a) Ga-2p level and (b) La-3d level of La-doped α-GaOOH nano-spindles.

Formation of gallium oxide nano-spindles

The structure of α-GaOOH consists of double chains of edge-sharing octahedra, and two-thirds of the octahedral interstices are occupied by gallium, whereas the oxygen-hydroxyl sheets form a hexagonal close-packed array.[21] The formation of α-GaOOH nano-spindles is not trivial, as it is well known that the orthorhombic phase exhibits shape anisotropy.[22] Our observations are in agreement with the results documented in the literature where preferential growth direction of undoped α-GaOOH was concluded to be [001], i.e., the *c*-axis.[23] Expectedly, at high pH, gallium hydroxide formation takes place rapidly along the [001] direction, which is energetically more favoured, and such a process lead to the formation of nano-spindles. However, after increasing the concentration of sodium azide from 0.1 M to 0.5 M, the morphology of the resulting spindle structures became less elongated, as evident from FESEM (**see ESI**). This could be presumably due to the adsorption of excess hydroxyl anions on surfaces other than those of high-energy, and is in agreement with the reports documented in the literature.[17] Morphological characterization reveals that increasing the concentration of sodium azide in the solution being sonicated leads to variation in size and morphology of α-GaOOH nano-spindles. The role of the sonic field was found to be critical and monodispersity in the size distribution remains conserved which could be due to the presence of sonic field everywhere in the irradiated solution.

HRTEM (**Fig. 3b & 4b**) revealed that numerous primary crystals are participating in oriented attachment, i.e., oriented growth occurs through the attachment of nuclei along a particular crystallographic orientation while as SAED (**Fig. 3c & 4c**) brought out that the nano-spindles are single-crystalline in nature. One could envisage such growth when there is rapid nucleation so that the process does not become diffusion-limited. As is known, diffusion-limited processes often lead to the formation of randomly oriented aggregates.[24] In principle, oriented aggregation is driven by the reduction of the overall energy resulting from the elimination of the surface energy associated with unsaturated bonding, i.e., the elimination of the various interfaces.[25]

In case of doped α-GaOOH, Ln^{3+} ions get inserted between the oxygen-hydroxyl sheets and it has been reported that, if the concentration of Ln^{3+} ion exceeds 1 at.%, the structure of nanorods collapses.[16] Surprisingly, we have been able to load the α-GaOOH nano-spindles with ~1.45 at.% La^{3+} ions without compromising with the shape of the nano-spindles. The retention of the morphology of nano-spindles after the transformation of La-doped α-GaOOH to La-doped β-Ga_2O_3 is remarkable as annealing at elevated temperature of 800 °C for more than 12 h could have distorted the morphology.

Photoluminescence Study

β-Ga_2O_3 exhibits a wide band gap of 4.9 eV at room temperature and has been reported as a visible blue-green light emitter.[26] Fig. 7 presents the room temperature photoluminescence spectra of undoped and La-doped β-Ga_2O_3 nano-spindles. Both the samples after dispersing in ethanol, were excited at 280 nm. The general features of the PL spectra are in good agreement with reports in the literature on β-Ga_2O_3 nanostructures.[26,27] It is seen that undoped and La-doped β-Ga_2O_3 nano-spindles exhibit strong broad-band emissions centered on 340 nm and 365 nm, respectively. The broad peaks ranging from 300 nm to 520 nm could be deconvoluted into several peaks, as displayed in the inset of Fig. 7. After deconvolution, it became quite evident that both the samples, i.e., undoped and La-doped β-Ga_2O_3, exhibit blue and green emission, in addition to UV emission. The origin of the UV emission could be due to the recombination of excitons, whereas blue emission has been attributed to the recombination of electrons on a donor states formed by oxygen vacancies, with the holes on acceptor states formed by gallium vacancies in β-Ga_2O_3.[28,29,30] Binet and Gourier documented a photoluminescence model for β-Ga_2O_3, wherein the blue emission originates from an excited hole on an acceptor

capturing an electron in a donor vacancy, resulting in the formation of a trapped exciton.[31] Additionally, a relatively less intense broad-band centered on 650 nm is also observed, which could be due to the recombination of electrons with the holes present in the sub-bands, or to the recombination of deeply trapped exciton.[32,33] The effect of La ions on the luminescence is quite evident, as a red shift of ~30 nm was observed in the UV emission of La-doped β-Ga_2O_3 relative the emission in undoped β-Ga_2O_3.

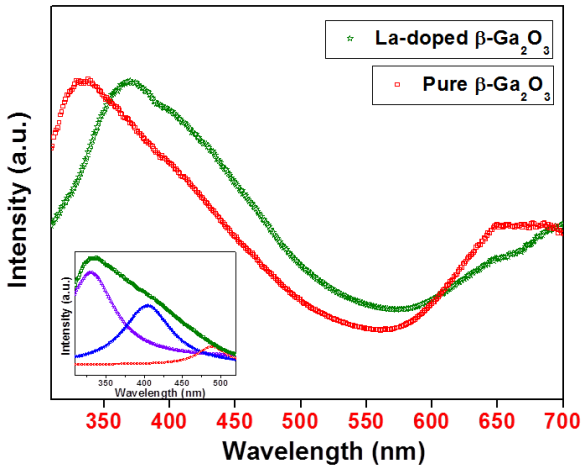

Fig. 7 Room temperature photoluminescence spectra of undoped and La-doped β-Ga_2O_3 nano-spindles

Conclusions

Nearly monodisperse undoped and La-doped α-GaOOH single crystalline nano-spindles with the dimension of ~550 nm were synthesized sonochemically without using any growth-directing agent. Controlled annealing under optimized conditions leads to the transformation of undoped and La-doped GaOOH nano-spindles, respectively, into nanostructures of α-Ga_2O_3 and β-Ga_2O_3. It is to be noted that these nano-spindles are single-crystalline and their growth could be explained by invoking the mechanism of oriented attachment. Retention of morphology of the gallium oxide nanostructures during structural transformations or after doping with lanthanide ions is remarkable and it could be attributed to the oriented attachment type of growth. Crystallinity, phase purity, and composition of as-prepared samples are thoroughly established by powder X-ray diffraction and electron microscopy (TEM and STEM). Moreover, the La^{3+} dopant evidently plays a role in influencing luminescence of La-doped β-Ga_2O_3 nano-spindles.

Experimental Section

Chemicals and sonochemical setup

An ultrasonic processor (SONIC Model VCX 500, 500 Watts) operating at 20 kHz, equipped with a solid Ti probe (13 mm dia), was used for the synthesis. The amplitude of ultrasonic waves was selected as 50% of the maximum, with a duty cycle of 60%. All chemicals were of the AR grade and used as-received. Gallium nitrate hydrated and lathanum nitrate hydrated were purchased, respectively, from Rankem and Sigma-Aldrich. Sodium azide (Sigma-Aldrich) and de-ionized (DI) water were used for the reaction. All the reactions were carried out in a fume hood.

Synthesis of gallium oxide nano-spindles

As summarized in the Table 1, different samples of undoped and La^{3+}-doped gallium oxide nano-spindles were prepared by conducting the sonication with the reaction mixture placed in an ice-bath. Typically, nano-spindles of α-GaOOH were synthesized by sonicating for 30 minutes the reaction mixture containing 15 mL of each 0.1 M gallium nitrate hydrated and 0.1 M sodium azide dissolved in DI water. Similarly, nano-spindles of La-doped *α*-GaOOH were synthesized after sonicating for 30 minutes the reaction mixture containing 14 mL 0.1 M gallium nitrate hydrated, 1 mL of 0.1 M lathanum nitrate hydrated, and 15 mL 0.1 M sodium azide dissolved in de-ionized water. A precipitate was separated from the supernatant by centrifugation at 4500 rpm for 15 min. No size-selective precipitation was carried out. The precipitate was washed twice with water, followed by drying under ambient conditions. Subsequently the formation of undoped and La-doped α-Ga_2O_3 and *β*-Ga_2O_3 was achieved by carrying out controlled annealing of respective *α*-GaOOH samples at elevated temperatures under optimized conditions (**Table 1)**.

Table 1 Summary of experimental conditions optimized for the synthesis of different gallium oxide nanostructures

Sample	Phases of gallium oxides	Experimental condition
Undoped	α-GaOOH	As-prepared
	α-Ga_2O_3	Obtained after annealing undoped α-GaOOH nano-spindles at 500 °C for 12 h under ambient conditions.
	β-Ga_2O_3	Obtained after annealing undoped *α*-Ga_2O_3 nano-spindles at 800 °C for 12 h under ambient conditions.
La-doped	α-GaOOH	As-prepared
	α-Ga_2O_3	Obtained after annealing La-doped α-GaOOH nano-spindles at 500 °C for 12 h under ambient conditions.
	β-Ga_2O_3	Obtained after annealing La-doped *α*-Ga_2O_3 nano-spindles at 800 °C for 12 h under ambient conditions.

Analysis and Measurements

The samples were examined by bright-field TEM, high-resolution TEM (HRTEM), STEM-EDS and selected-area electron diffraction (SAED) in a JEOL JEM-2100F microscope operating at an accelerating voltage of 200 kV, equipped with an Oxford energy-dispersive X-ray (EDX) detector. The TEM specimens were prepared by slow evaporation of diluted solutions, obtained by dispersion of powders in ethanol, and deposited on a formvar-coated copper grid. A field-emission scanning electron microscope (FESEM, Carl Zeiss ULTRA 55) with EDS was employed to analyze the morphology of samples. An electron beam accelerated to 10 kV was used with an in-lens detector. FESEM samples were prepared by dispersing the powder onto a carbon tape and mounting it on an aluminum specimen holder. Powder X-ray diffraction (XRD) data were

collected on a Bruker Advance D8 X-ray diffractometer with a graphite monochromator, using Cu-K_α radiation, at a scanning rate of 0.2 deg min^{-1}. Photoluminescence data were collected at room temperature using a Perkin Elmer Lambda 700 UV-Vis-near-IR spectrophotometer with a double monochromator optical system. Photoluminescence (PL) spectra of undoped and La-doped gallium oxide nano-spindles were obtained with excitation at 280 nm using a xenon lamp. X-ray photoelectron spectra (XPS) were recorded on a Thermoscientific Multilab 2000 equipment, using Mg-K_α X-rays as the source (hν =1253.4 eV).

Acknowledgements

M.I.D thanks the UGC for a fellowship. We thank the Institute Nanoscience Initiative (IISc.) for allowing us to access the microscopy facilities, and the Micro and Nano Characterization Facility (MNCF) located at CeNSE, IISc, (funded by NPMAS-DRDO and MCIT, Government of India) for various analyses. We also thank the Indian Institute of Science for funding the procurement of a 200 kV TEM.

Notes and references

[a] Centre for Nano Science and Engineering, Indian Institute of Science, Bangalore 560012, India. E-mail: shivu@cense.iisc.ernet.in; Fax: +91 80 2360 4656; Tel: +9180 2293 3323
[b] Materials Research Centre, Indian Institute of Science, Bangalore 560012, India.
[c] Department of Inorganic & Physical Chemistry, Indian Institute of Science, Bangalore 560012, India.

Electronic Supplementary Information (ESI) available: [PXRD patterns of pure gallium oxide nano-spindles, TEM data of annealed samples, and FESEM data of α-GaOOH]. See DOI: 10.1039/b000000x/

1 M. Fleischer and H. Meixner, *Sens. Actuators B*, 1991, **4**, 437-441.
2 A. L. Petre, A. Auroux, P. Gélin, M. Caldararu and N. I. Ionescu, *Thermochim. Acta*, 2001, **379**, 177-185.
3 T. Miyata, T. Nakatani and T. Minami, *J. Lumin.*, 2000, **87**, 1183.
4. R. Roy, V. G. Hill and E. F. Osborn, *J. Am. Chem. Soc.*, 1952, **74**, 719-722.
5 Y. Zhao, R. L. Frost, J. Yang and W. N. Martens, *J. Phys. Chem. C*, 2008, **112**, 3568-3579.
6 A. W. Laubengayer and H. R. Engle, *J. Am. Chem. Soc.*, 1939, **61**, 1210-1214.
7 A. C. Taş, P. J. Majewski and F. Aldinger, *J. Am. Ceram. Soc.*, 2002, **85**, 1421-1429.
8 M. Ristić, S. Popović and S. Musić, *Mater. Lett.*, 2005, **59**, 1227-1233.
9 S. Fujihara, Y. Shibata and E. Hosono, *J. Electrochem. Soc*. 2005, **152**, C764.
10 Avivi, S.; Mastai, Y.; Hodes, G.; Gedanken, A. *J. Am. Chem. Soc*. 1999, **121**, 4196.
11 D. Kisailus, J. H. Choi, J. C. Weaver, W. Yang and D. E. Morse, *Adv. Mater*., 2005, **17**, 314-318.
12 H. Xu, B. W. Zeiger and K. S. Suslick, *Chem. Soc. Rev.*, 2013, **42**, 2555-2567.
13 *(a)* K. S. Suslick, *Science*, 1990, **247**, 1439-1445; *(b)* E. B. Flint and K. S. Suslick, *Science*, 1991, **253**, 1397-1399.
14 Y. Zhao, R. L. Frost, W. N. Martens, *J. Phys. Chem. C* 2007, **111**, 16290.
15 *(a)* P. Gollakota, A. Dhawan, P. Wellenius, L. M. Lunardi, J. F. Muth, Y. N. Saripalli, H. Y. Peng and H. O. Everitt, *Appl. Phys. Lett.*, 2006, **88**, 221906; *(b)* L. Fu, Z. Liu, Y. Liu, B. Han, J. Wang, P. Hu, L. Cao and D. Zhu, *J. Phys. Chem. B*, 2004, **108**, 13074-13078; *(c)* M. L. Pang, W. Y. Shen and J. Lin, *J. Appl. Phys.*, 2005, **97**, 033511; *(d)* T. Biljan, A. Gajović and Z. Meić, *J. Lumin.*, 2008, **128**, 377-382; *(e)* Nogales, E.; Mendez, B.; Piqueras, J. E. Nogales, B. Méndez and J. Piqueras, *Nanotechnology*, 2008, **19**, 035713; *(f)* E. Nogales, B. Méndez, J. Piqueras and J. A. García, *Nanotechnology*, 2009, **20**, 115201; *(g)* H. Xie, L. Chen, Y. Liu and K. Huang, *Solid State Commun.*, 2007, **141**, 12-16.
16 B. Sanyasi Naidu, M. Pandey, J. Nuwad, V. Sudarsan, R. K. Vatsa, R. J. Kshirsagar and C. G. S. Pillai, *Inorg. Chem.*, 2011, **50**, 4463-4472.
17 G. Li, C. Peng, C. Li, P. Yang, Z. Hou, Y. Fan, Z. Cheng and J. Lin, *Inorg. Chem.*, 2010, **49**, 1449-1457.
18 A. C. Taş, P. J. Majewski and F. Aldinger, *J. Am. Ceram. Soc.*, 2002, **85**, 1421-1429.
19 J. S. Trevor, P. H. Daniel, Z. Xiaobo, B.-S. Mariela, H. Myung Gwan, L. p.-L. Edgar, J. L. Robert, M. A. Pulickel, N.-C. Hugo and A. V. Miguel, *Nanotechnology*, 2012, **23**, 325601.
20 *(a)* C. K. Jørgensen and H. Berthou, *Chem. Phys. Lett.*, 1972, **13**, 186-189; *(b)* M. F. Sunding, K. Hadidi, S. Diplas, O. M. Løvvik, T. E. Norby and A. E. Gunnæs, *J. Electron. Spectrosc. Relat. Phenom.*, 2011, **184**, 399-409.
21 S. Yan, L. Wan, Z. Li, Y. Zhou and Z. Zou, *Chem. Commun.*, 2010, **46**, 6388-6390.
22 R. Hill, *Phys. Chem. Miner.*, 1979, **5**, 179-200
23 *(a)* C.-C. Huang, C.-S. Yeh and C.-J. Ho, *J. Phys. Chem. B*, 2004, **108**, 4940-4945; *(b)* H.-S. Qian, P. Gunawan, Y.-X. Zhang, G.-F. Lin, J.-W. Zheng and R. Xu, *Cryst. Growth Des., 2008, **8**, 1282-1287.*
24 Y. Zhou and M. Antonietti, *J. Am. Chem. Soc.*, 2003, **125**, 14960-14961.
25 *(a)* 71 R. L. Penn and J. F. Banfield, *Science*, 1998, **281**, 969-971; *(b)* 12 R. L. Penn, *J. Phys. Chem. B*, 2004, **108**, 12707-12712; *(c)* M. I. Dar, A. K. Chandiran, M. Gratzel, M. K. Nazeeruddin and S. A. Shivashankar, *J Mater. Chem.A*, 2014, **2**, 1662-1667; *(d)* M. I. Dar, S. Sampath and S. A. Shivashankar, *J. Mater. Chem.*, 2012, **22**, 22418-22423; *(e)* M. I. Dar, S. Sampath and S. A. Shivashankar, *Mater. Res. Express* , 2014, **1**, 015025.
26 S. C. Vanithakumari and K. K. Nanda, *Adv. Mater.*, 2009, **21**, 3581-3584.
27 K. W. Chang and J. J. Wu, *Adv. Mater.*, 2004, **16**, 545-549.
28 V. i. Vasiltsiv, Y. M. Zakharko and Y. I. Prim, *Ukr. Fiz. Zh.* 1988, **33**, 1320.
29 T. Harwig and F. Kellendonk, *J. Solid State Chem.*, 1978, **24**, 255-263.
30 C.-C. Huang and C.-S. Yeh, *New J. Chem.*, 2010, **34**, 103-107.
31 L. Binet and D. Gourier, *J. Phys. Chem. Solids*, 1998, **59**, 1241-1249.
32 X. T. Zhou, F. Heigl, J. Y. P. Ko, M. W. Murphy, J. G. Zhou, T. Regier, R. I. R. Blyth and T. K. Sham, *Phys. Rev. B*, 2007, **75**, 125303.
33 Y. P. Song, H. Z. Zhang, C. Lin, Y. W. Zhu, G. H. Li, F. H. Yang and D. P. Yu, *Phys. Rev. B*, 2004, **69**, 075304;